




# Quantitative MRI Reveals Microstructural Changes in the Upper Leg Muscles After Running a Marathon

Melissa T. Hooijmans, PhD,<sup>1\*</sup>  Jithsa R.C. Monte, MD,<sup>2</sup> Martijn Froeling, PhD,<sup>3</sup>   
Sandra van den Berg-Faay, MSc,<sup>2</sup> Vincent L. Aengevaeren, MD,<sup>4,5</sup> Robert Hemke, MD,<sup>2</sup>  
Frank F. Smithuis, MD,<sup>2</sup> Thijs M.H. Eijsvogels, PhD,<sup>4</sup> Adrianus J. Bakermans, PhD,<sup>2</sup>   
Mario Maas, MD, PhD,<sup>2</sup> Aart J. Nederveen, PhD,<sup>2</sup> and Gustav J. Strijkers, PhD<sup>1</sup>

**Background:** The majority of sports-related injuries involve skeletal muscle. Unlike acute trauma, which is often caused by a single traumatic event leading to acute symptoms, exercise-induced microtrauma may remain subclinical and difficult to detect. Therefore, novel methods to detect and localize subclinical exercise-induced muscle microtrauma are desirable.

**Purpose:** To assess acute and delayed microstructural changes in upper leg muscles with multiparametric quantitative MRI after running a marathon.

**Study Type:** Longitudinal; 1-week prior, 24–48 hours postmarathon and 2-week follow-up

**Population:** Eleven men participants (age: 47–68 years).

**Field Strength/Sequence:** Spin-echo echo planar imaging (SE-EPI) with diffusion weighting, multispin echo, Dixon, and fat-suppressed turbo spin-echo (TSE) sequences at 3T. MR datasets and creatine kinase (CK) concentrations were obtained at three timepoints.

**Assessment:** Diffusion parameters, perfusion fractions, and quantitative (q)T<sub>2</sub> values were determined for hamstring and quadriceps muscles, TSE images were scored for acute injury. The vastus medialis and biceps femoris long head muscles were divided and analyzed in five segments to assess local damage.

**Statistical Tests:** Differences between timepoints in MR parameters were assessed with a multilevel linear mixed model and in CK concentrations with a Friedman test. Mean diffusivity (MD) and qT<sub>2</sub> for whole muscle and muscle segments were compared using a multivariate analysis of covariance (MANCOVA).

**Results:** CK concentrations were elevated (1194 U/L [166–3906],  $P < 0.001$ ) at 24–48 hours postmarathon and returned to premarathon values (323 U/L [56–2216]) at 2-week follow-up. Most of the MRI diffusion indices in muscles without acute injury changed at 24–48 hours postmarathon and returned to premarathon values at follow-up (MD, RD, and  $\lambda$ 3;  $P < 0.006$ ). qT<sub>2</sub> values ( $P = 0.003$ ) and perfusion fractions ( $P = 0.003$ ) were higher at baseline compared to follow-up. Local assessments of MD and qT<sub>2</sub> revealed more pronounced changes than whole muscle assessment (2–3-fold;  $P < 0.01$ ).

**Data Conclusion:** Marathon running-induced microtrauma was detected with MRI in individual whole upper leg muscles and even more pronounced on local segments.

**Level of Evidence:** 2

**Technical Efficacy Stage:** 3

J. MAGN. RESON. IMAGING 2020;52:407–417.

**S**KELETAL MUSCLE INJURIES are the most prevalent injuries in recreational and elite sports.<sup>1</sup> Acute trauma, such as muscle tears or ruptured tendons, may result from a single traumatic event or forceful blow. Microtrauma (overuse) injury may result from repetitive use of muscles.<sup>2</sup> Whereas acute trauma commonly has a clear clinical presentation, the diagnosis

View this article online at [wileyonlinelibrary.com](http://wileyonlinelibrary.com). DOI: 10.1002/jmri.27106

Received Sep 10, 2019, Accepted for publication Feb 13, 2020.

\*Address reprint request to: M.H., Meibergdreef 9, 1105 AZ AMSTERDAM, The Netherlands, E-mail: [m.t.hooijmans@amsterdamumc.nl](mailto:m.t.hooijmans@amsterdamumc.nl)

From the <sup>1</sup>Amsterdam University Medical Centers, University of Amsterdam, Department of Biomedical Engineering and Physics, Amsterdam Movement Sciences, Amsterdam, Netherlands; <sup>2</sup>Amsterdam University Medical Centers, University of Amsterdam, Department of Radiology and Nuclear Medicine, Amsterdam Movement Sciences, Amsterdam, Netherlands; <sup>3</sup>Department of Radiology, University Medical Center Utrecht, Utrecht, Netherlands; <sup>4</sup>Radboud Institute for Health Sciences, Department of Physiology, Radboud University Medical Center, Nijmegen, Netherlands; and <sup>5</sup>Radboud Institute for Health Sciences, Department of Cardiology, Radboud University Medical Center, Nijmegen, Netherlands

This is an open access article under the terms of the Creative Commons Attribution-NonCommercial License, which permits use, distribution and reproduction in any medium, provided the original work is properly cited and is not used for commercial purposes.

**TABLE 1. Scan Parameters for qT<sub>2</sub>, DWI, Dixon, and Fat-Suppressed T<sub>2</sub>-Weighted Sequences**

	qT <sub>2</sub>	DWI	Noise map	Dixon	T <sub>2</sub> w-SPIR
Sequence	MSE	SE-EPI	SE-EPI	MS_FFE	MS_TSE
Matrix size	160 × 160	160 × 160	160 × 160	320 × 320	640 × 640
Voxel size (mm <sup>3</sup> )	3 × 3 × 6	3 × 3 × 6	3 × 3 × 6	1.5 × 1.5 × 6	0.75 × 0.75 × 3
Slice gap (mm)	6	—	—	—	—
Slices	17	31	31	31	31
TR (msec)	5633	5000		210	5500
TE (msec)	17*7.6	57	57	2.6/3.36/ 4.12/4.88	70
Flip angle	90/180°	90/180°	90/180°	8°	90°
b-value (s/mm <sup>2</sup> ) (# gradient orientations)	—	0(1), 1(6), 10(3), 25(3), 100(3), 200(6), 400(8), 600(12)	0(1), 400(1)	—	—
Fat suppression		SPAIR/SPIR/SSGR	SPAIR/SPIR/SSGR		SPIR
SENSE	2	1.9	1.9	2	2

SENSE: sensitivity encoding.

of subclinical microtrauma is difficult. Under healthy physiological conditions, exercise-induced muscle microtrauma is efficiently repaired, requiring minimal or no treatment.<sup>3</sup> Repetitive microtrauma, however, may cause complications and eventually result in injury.<sup>4</sup> Therefore, a need exists for imaging methods to detect and localize subclinical muscle microtrauma.

Currently, fat-suppressed T<sub>2</sub>-weighted magnetic resonance imaging (MRI) assists in the diagnosis of muscle injury, but this technique fails to detect microtrauma and has a limited ability to predict recovery.<sup>5-8</sup> Quantitative MRI techniques, including diffusion tensor imaging (DTI) and

quantitative T<sub>2</sub> (qT<sub>2</sub>), have shown promise for the detection of microtrauma and for monitoring recovery.<sup>5,8-11</sup> For example, DTI was able to detect changes in muscle microstructure after running a marathon on a level that remained undetected with regular fat-suppressed T<sub>2</sub>-weighted MRI.<sup>5</sup> qT<sub>2</sub> has been applied to detect exercise-induced changes in muscle and to monitor recovery of muscle injury.<sup>12-14</sup>

The interpretation of changes in DTI and qT<sub>2</sub> with muscle exercise, injury, and recovery can be challenging, because diffusion indices can change due to several different (pathological) processes including inflammation, cell swelling,

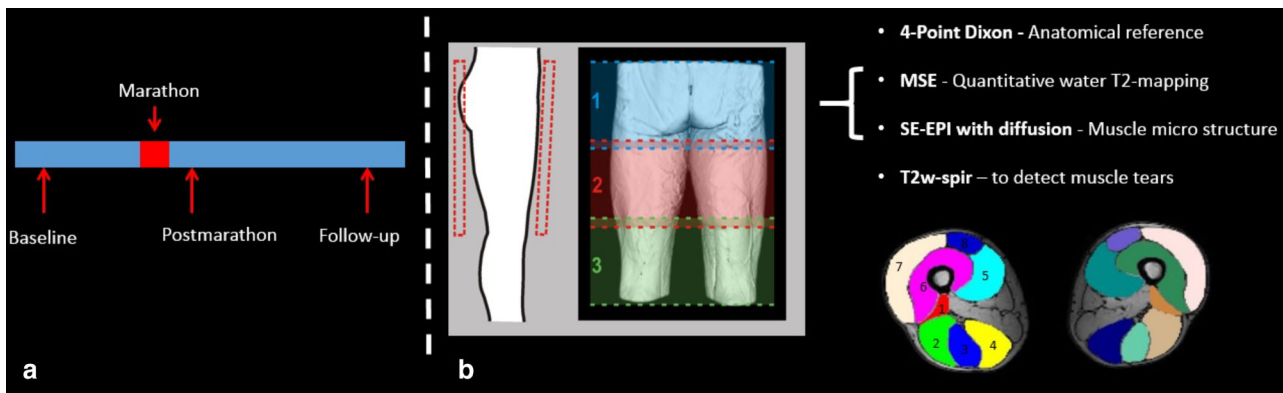


**FIGURE 1: Study design. (a)** Timeline indicating marathon and timepoints of MRI and blood sampling. **(b)** Schematic view of the scan geometry with three stacks of 31 slices and 30 mm section overlap covering the upper legs. Bottom right: Dixon images at mid-thigh level with manually drawn ROIs for eight upper leg muscles: 1 = BFS, 2 = BFL, 3 = ST, 4 = SM, 5 = VM, 6 = VI, 7 = VL, 8 = RF.

and atrophy.<sup>15,16</sup> Moreover, diffusion indices might be contaminated by muscle perfusion and changes therein.<sup>17</sup> Similarly,  $T_2$  relaxation times can be altered by a wide range of physiological modifications, and are suggested to be at least partly driven by osmotic changes that are potentially indicative of inflammation and edema.<sup>11,18</sup> Consequently, a single MRI readout is not sufficient to characterize muscle injury and repair, and a multiparametric MRI readout might be required. Moreover, the muscle's vulnerability to injury depends on specific muscle function and structure. Both these aspects of skeletal muscle are not homogeneously distributed within individual muscles and require local analysis.<sup>19–22</sup>

The goal of this study was to implement a multiparametric MRI protocol to characterize exercise-induced microtrauma and recovery in individual whole upper leg muscles and on a local muscle level.

## Materials and Methods

The study was approved by the local Medical Ethical Committee and all participants signed a written informed consent.

### Participants and Study Flow

Twelve participants were recruited, based on the inclusion criteria that participants were older than 45 years without any cardiovascular (CV) diseases or risk factors, had no MRI contraindications, no acute injury or diagnosed muscle disease, and had completed at least one marathon (42.195 km road race) prior to participating in this study. The participants competed in the marathon of Amsterdam (The Netherlands) on October 15, 2017. MRI datasets and venous blood samples were obtained at three timepoints: 1) baseline (1 week prior to the marathon), 2) postmarathon (24–48 hours after the marathon), and 3) follow-up (2 weeks postmarathon). At the baseline visit, all participants completed a questionnaire about personal characteristics, including health status (medication history and medication use), marathon experience (personal record, previous completed marathons), and lifelong exercise history.<sup>23</sup> Participants were asked to restrain from any extensive exercise 48 hours prior to the scans, but received no instructions for their training regime prior to and postmarathon.

**TABLE 2. Baseline Subject Characteristics of the 11 Marathon Finishers**

Subject characteristics	Mean $\pm$ SD
Age (years)	51 $\pm$ 6
Previous marathons ( <i>n</i> )	13 $\pm$ 7
Height (cm)	180 $\pm$ 7
BMI, kg/m <sup>2</sup>	23.6 $\pm$ 1.1
Weight (kg)	76.9 $\pm$ 7.2
Finish time (min)	236 $\pm$ 35

### MRI Protocol

Participants received an MRI examination of both upper legs with a 3T MR scanner (Ingenia, Philips, Best, Netherlands) using a 16-element anterior body receive coil and a 12-channel table top coil and were positioned in a feet-first supine position in the scanner. The data were acquired in three transverse stacks with 30 mm overlap, covering 498 mm proximal to distal with a field of view (FOV) of 480  $\times$  276 mm<sup>2</sup>. The total duration of the scan protocol was 48 minutes and included a diffusion-weighted spin-echo echo planar imaging (SE-EPI) for DTI parameters and perfusion fractions, SE-EPI without diffusion weighting to quantify signal to noise ratios (SNRs), a multiturbo spin echo sequence for quantitative water  $T_2$  mapping ( $qT_2$ ), a Dixon sequence for anatomical reference, and a fat-suppressed  $T_2$ -weighted scan to assess acute muscle injury (see Table 1).<sup>24</sup>

### MRI Data Analysis

MR images were analyzed using QMRITools for Mathematica (<https://mfroeling.github.io/QMRITools>). Diffusion data were denoised using a principle component analysis (PCA) noise algorithm, and spatially registered to correct for motion and eddy currents-induced displacements using an affine registration in an open-source registration tool (<http://etastix.isi.uu.nl>). Second, the diffusion data were corrected for EPI distortions by registering to anatomical space using a rigid registration and a B-spline registration. The diffusion tensor was calculated using an intravoxel incoherent motion (IVIM)-based iterative weighted linear least squares algorithm (iWLLS).<sup>25</sup> By using IVIM correction, an anisotropic pseudodiffusion component was modeled in addition to the standard diffusion tensor, to remove the perfusion biases in the diffusivity estimation.<sup>24</sup> The eigenvalues ( $\lambda_1$ ,  $\lambda_2$ ,  $\lambda_3$ ), mean diffusivity (MD), fractional anisotropy (FA), and the pseudoperfusion fractions were used as outcome parameters. Quantitative  $T_2$  maps were calculated using an extended phase graph (EPG) fit, considering different relaxation times for the water and fat signal components.<sup>26</sup> This method partitions magnetization into coherence pathways to accurately compute the amplitudes of each of the signals. The fat  $T_2$  relaxation time was independently obtained from the subcutaneous fat for each subject and subsequently fixed during fitting. Water  $T_2$  relaxation times and B1+ values were determined per voxel using a dictionary method.

The  $T_2$ -weighted images with fat suppression were graded by three musculoskeletal radiologists (M.M., >25 years' experience in evaluation of musculoskeletal MRI; F.S., 3 years' experience; and R.H., 2 years' experience) for acute muscle injury using a standardized grading system.<sup>27</sup> Signs of muscle injury were graded as 0, 1, 2, or 3, with 0 = no abnormalities, 1 = mild swelling and edema without discontinuities of the muscle tissue, 2 = partially ruptured muscle tissue and presence of edema, and 3 = complete disruption of the muscle tissue. The radiologists were not blinded for the different timepoints or participants, which is in accordance with clinical practice in our hospital. Muscles with insufficient SNR (<15)<sup>28</sup> or graded for acute injury (1 < radiologists) were excluded from further analysis.<sup>5</sup>

Eight muscles in both upper legs, ie, biceps femoris short head (BFS), biceps femoris long head (BFL), semitendinosus (ST), semimembranosus (SM), vastus medialis (VM), vastus lateralis (VL), vastus intermedius (VI), and rectus femoris (RF) muscles, were

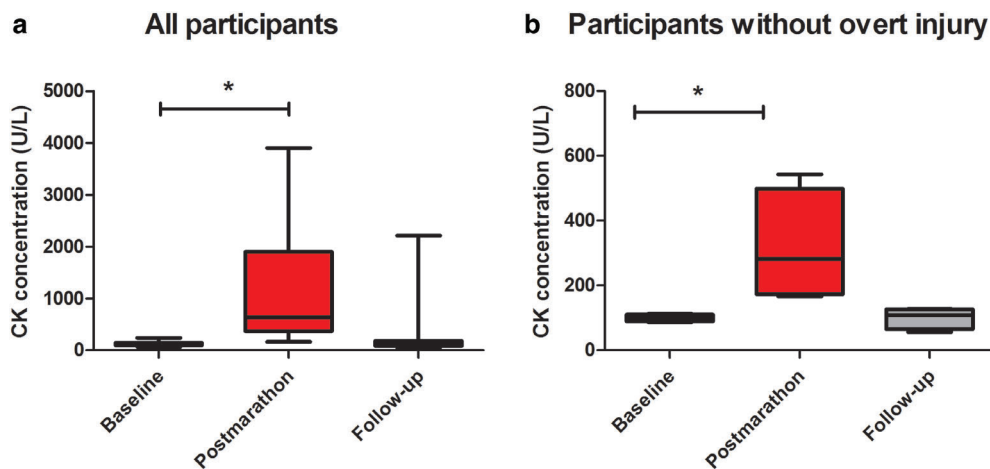


FIGURE 2: Boxplots showing the CK concentrations (U/L) in the venous blood for all participants at baseline, postmarathon, and follow-up (a) showing all participants and (b) with exclusion of participants with overt injuries. Significant differences are indicated with an asterisk (\*).

manually segmented based on the out-of-phase Dixon images (ITK-snap, Fig. 1b) avoiding fascia and subcutaneous fat tissue. Segmentations were smoothed and eroded by one pixel to avoid partial volume effects with fat tissue. The segmentations were subsequently registered to the  $qT_2$  and DTI maps. Outcome parameters are reported as mean values for each individual muscle.

Muscle injury in recreational and elite sports is most frequently seen in the BFL muscle, but not so often in the VM muscle.<sup>1,29,30</sup> We therefore chose these two muscles for a more detailed local evaluation of MD and  $qT_2$ . To this end, both muscles were proximally to distally segmented in five equal sections (meaning equal number of slices). For each segment, both the absolute and

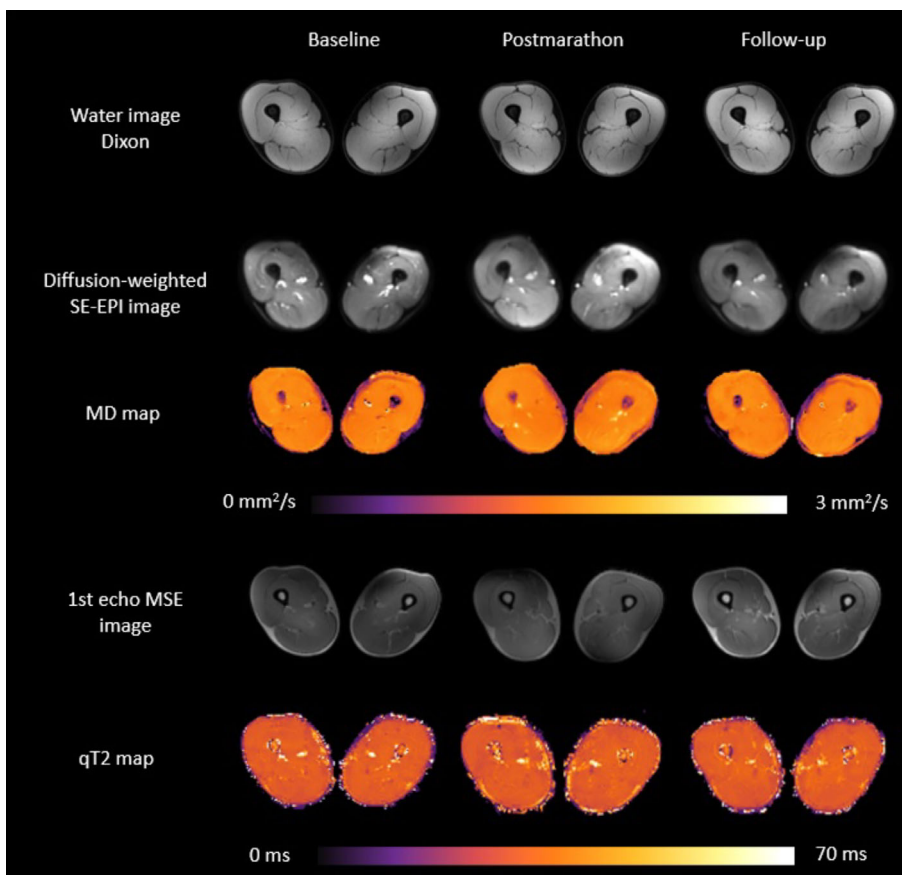


FIGURE 3: Raw and processed example images of a representative subject (47 years/male) for the three timepoints. Left column: baseline, middle column: postmarathon and right column: follow-up. Top: water images from Dixon sequence. Middle: raw diffusion images for  $b = 0 \text{ s/mm}^2$  and MD maps. Bottom: raw images from first TE of  $T_2$  sequence and processed EPG  $T_2$  maps.

**TABLE 3. Mean and Standard Deviations for the Diffusion Parameters, Per Muscle, Per Timepoint**

Muscle	Timepoint	$\lambda_1$ (mm <sup>2</sup> /sec)	$\lambda_2$ (mm <sup>2</sup> /sec)	$\lambda_3$ (mm <sup>2</sup> /sec)	MD (mm <sup>2</sup> /sec)	FA(-)	RD (mm <sup>2</sup> /sec)	Perfusion fraction (%)	Water T <sub>2</sub> values (msec)
<b>Hamstrings</b>									
BFS	1	1.96 ± 0.09	1.47 ± 0.09	1.26 ± 0.05	1.56 ± 0.06	0.23 ± 0.03	1.36 ± 0.07	0.042 ± 0.02	30.6 ± 1.2
	2	1.96 ± 0.13	1.43 ± 0.1	1.25 ± 0.1	1.55 ± 0.1	0.23 ± 0.02	1.34 ± 0.1	0.043 ± 0.01	30.7 ± 1.1
	3	1.93 ± 0.14	1.42 ± 0.09	1.25 ± 0.08	1.54 ± 0.08	0.23 ± 0.03	1.33 ± 0.08	0.037 ± 0.02	30.2 ± 1.2
BFL	1	1.97 ± 0.08	1.54 ± 0.05	1.33 ± 0.05	1.62 ± 0.05	0.20 ± 0.03	1.44 ± 0.04	0.03 ± 0.01	30.2 ± 1.1
	2	1.99 ± 0.07	1.56 ± 0.05	1.37 ± 0.06**	1.64 ± 0.04**	0.19 ± 0.02	1.47 ± 0.04**	0.024 ± 0.004	30.05 ± 0.8
	3	1.95 ± 0.07	1.52 ± 0.04	1.35 ± 0.05	1.61 ± 0.04	0.19 ± 0.03	1.43 ± 0.04	0.024 ± 0.01	29.8 ± 0.8
ST	1	1.99 ± 0.06	1.50 ± 0.06	1.41 ± 0.05	1.62 ± 0.05	0.21 ± 0.02	1.43 ± 0.05	0.03 ± 0.01	29.1 ± 1.1
	2	2.04 ± 0.06	1.54 ± 0.05	1.37 ± 0.04**	1.66 ± 0.05**	0.20 ± 0.01	1.47 ± 0.05**	0.03 ± 0.01	29.1 ± 1.3
	3	1.99 ± 0.07	1.50 ± 0.05	1.36 ± 0.05	1.63 ± 0.04	0.20 ± 0.02	1.44 ± 0.05	0.03 ± 0.01	28.7 ± 0.9
SM	1	1.86 ± 0.06	1.48 ± 0.06	1.31 ± 0.04	1.55 ± 0.05	0.18 ± 0.02	1.40 ± 0.05	0.039 ± 0.01	30.1 ± 1.1
	2	1.87 ± 0.05	1.48 ± 0.06	1.33 ± 0.05	1.56 ± 0.05	0.19 ± 0.02	1.41 ± 0.06	0.036 ± 0.01	30.0 ± 1.0
	3	1.85 ± 0.07	1.48 ± 0.08	1.32 ± 0.06	1.55 ± 0.06	0.18 ± 0.01	1.40 ± 0.07	0.032 ± 0.01	29.9 ± 1.3
<b>Quadriceps</b>									
VM	1	1.82 ± 0.04	1.44 ± 0.05	1.29 ± 0.05	1.52 ± 0.04	0.18 ± 0.02	1.37 ± 0.04	0.04 ± 0.01	30.5 ± 0.9
	2	1.84 ± 0.04	1.48 ± 0.05	1.35 ± 0.04**	1.56 ± 0.03**	0.16 ± 0.02	1.41 ± 0.04**	0.04 ± 0.004	30.4 ± 0.9
	3	1.81 ± 0.06	1.46 ± 0.04	1.32 ± 0.05	1.54 ± 0.04	0.17 ± 0.02	1.39 ± 0.05	0.03 ± 0.01	30.4 ± 0.7
VL	1	1.94 ± 0.05	1.56 ± 0.06	1.39 ± 0.05	1.63 ± 0.05	0.17 ± 0.01	1.48 ± 0.05	0.04 ± 0.01	30.4 ± 0.9
	2	1.96 ± 0.03	1.59 ± 0.04	1.43 ± 0.04**	1.65 ± 0.03**	0.16 ± 0.01	1.51 ± 0.04**	0.03 ± 0.01	30.4 ± 0.9
	3	1.93 ± 0.03	1.56 ± 0.05	1.39 ± 0.05	1.63 ± 0.04	0.17 ± 0.02	1.47 ± 0.05	0.04 ± 0.01	30.3 ± 0.6
VI	1	1.92 ± 0.05	1.57 ± 0.05	1.38 ± 0.05	1.63 ± 0.05	0.17 ± 0.02	1.48 ± 0.05	0.03 ± 0.01	30.1 ± 0.8
	2	1.94 ± 0.03	1.59 ± 0.04	1.43 ± 0.05**	1.65 ± 0.03**	0.16 ± 0.02	1.51 ± 0.04**	0.03 ± 0.01	30.3 ± 0.9
	3	1.91 ± 0.05	1.56 ± 0.04	1.38 ± 0.05	1.62 ± 0.04	0.17 ± 0.02	1.47 ± 0.04	0.03 ± 0.01	29.9 ± 0.7
RF	1	1.83 ± 0.1	1.42 ± 0.1	1.23 ± 0.09	1.50 ± 0.02	0.20 ± 0.02	1.33 ± 0.09	0.04 ± 0.02	29.1 ± 0.9
	2	1.84 ± 0.1	1.46 ± 0.08	1.28 ± 0.09	1.53 ± 0.09	0.19 ± 0.02	1.37 ± 0.09	0.04 ± 0.01	29.0 ± 1.1
	3	1.84 ± 0.3	1.39 ± 0.15	1.19 ± 0.2	1.47 ± 0.16	0.22 ± 0.09	1.29 ± 0.16	0.04 ± 0.02	29.1 ± 0.8

BFS: Biceps Femoris Short Head, BFL: Biceps Femoris Long Head, ST: Semitendinosus, SM: Semimembranosus, VM: Vastus Medialis, VL: Vastus Lateralis, VI: Vastus Intermedius and RF: Rectus Femoris.  $\lambda_1$ : First eigenvalue,  $\lambda_2$ : Second eigenvalue,  $\lambda_3$ : Third eigenvalue. MD: Mean Diffusivity, FA: Fractional Anisotropy, RD: Radial Diffusivity. Differences between baseline and postmarathon are indicated with an asterisk (\*). Differences between postmarathon and follow-up are indicated with a number sign (#).

relative difference (delta,  $\Delta$ ) were determined between baseline and postmarathon values.

### Creatine Kinase Measurements

At each MR session, a venous blood sample (4.5 mL in a lithium-heparin tube) was collected to measure circulating plasma concentrations of CK using a standard enzymatic assay by the same lab.

### Statistical Analysis

Differences in DTI parameters and  $qT_2$  values between timepoints were assessed with a multilevel linear mixed model as an overall time-effect per outcome parameter. The level of statistical significance was corrected for multiple comparisons (eight outcome measures [ $0.05/8 = 0.006$ ]) and set at  $P < 0.006$ . Additionally, age was included in the model as a continuous predictor variable to account for a potential age effect. A post-hoc analysis was used to determine the contributions of the individual muscles to the main time effect. A multivariate analysis of covariance (MANCOVA) was used to compare whole muscle and local measurements of MD and  $qT_2$  values in BFL and VM muscles. The significance level was set at  $P < 0.05$ . Lastly, differences in CK concentrations over time were assessed with a Friedman test.

## Results

### Participant Characteristics

One out of the 12 participants did not finish the marathon and was therefore excluded from further analysis. The remaining 11 participants finished the race in an average time of  $236 \pm 35$  minutes, had completed 13 marathons<sup>2–25</sup> in the past, and had a lifelong exercise volume of 22 (7.91–62.26) metabolic equivalent of task hours per week. Additional participant and race characteristics are given in Table 2.

### Radiological Scoring/CK Concentrations

None of the participants had any acute muscle injury at baseline. Postmarathon, all participants reported muscle soreness and a sense of stiffness but only 27 acute injuries were detected in muscles of six participants (BFS = 2, BFL = 2, ST = 3, SM = 1, VM = 4, VI = 8, VL = 5, and RF = 2). At the 2-week timepoint, 11 acute injuries were observed in muscles of five participants (BFL = 1, ST = 2, VM = 2, VL = 2, VI = 3, and RF = 1), of which three were new ones (BFL, VL, and RF) and the others were recovering acute injuries identified at the postmarathon timepoint. Median CK concentrations of all participants were 121 U/L (69–238) at baseline, which increased 10-fold to 1194 U/L (166–3901) at 24–48 hours postmarathon, and decreased to 323 U/L (56–2216) at follow-up (Fig. 2a). After exclusion of CK concentrations of participants with acute muscle injury, the increase directly after the marathon was less pronounced (3.5-fold), with 121 U/L (69–238) at baseline, 401 U/L (166–732) at the postmarathon timepoint, and 126 U/L (56–180) at follow-up (Fig. 2b). Two participants took some pain medication (paracetamol, 1000 mg, or 4 ibuprofen) postmarathon.

### Quantitative MRI Parameters

Multiparametric MR images and quantitative parameter maps of a representative participant at all three timepoints are shown in Fig. 3. From the 528 analyzed muscles of all participants at all timepoints, 51 muscles had to be excluded due to acute injury ( $n = 38$ ) or low SNR ( $n = 13$ ; BFS = 7, SM = 3, RF = 3).

Mean values and standard deviations of all outcome parameters for the three timepoints per muscle are summarized in Table 3. An overall time-effect was found for the diffusion indices RD ( $P = 0.006$ ), MD ( $P = 0.0001$ ), and  $\lambda_3$  ( $P = 0.002$ ) (Fig. 4). Post-hoc analysis showed that the BFS, SM, and RF muscles did not contribute to this time-effect for any of the outcome measures. For all five other upper leg muscles, ie, BFL ( $P = 0.002$ ), ST ( $P = 0.001$ ), VM ( $P = 0.0004$ ), VI ( $P = 0.001$ ), VL ( $P = 0.0001$ ),  $\lambda_3$  was higher postmarathon compared to both baseline and follow-up.

Similarly, MD was higher postmarathon compared to baseline and follow-up in the BFL ( $P = 0.021$ ), ST ( $P = 0.003$ ), VM ( $P = 0.001$ ), VI ( $P = 0.002$ ), and VL ( $P = 0.003$ ). RD was higher postmarathon compared to baseline and follow-up in BFL ( $P = 0.014$ ), ST ( $P = 0.001$ ), VM ( $P = 0.0002$ ), VI ( $P = 0.001$ ), and VL ( $P = 0.001$ ). MD and RD values in BFL and VI muscles were only elevated postmarathon compared to follow-up but not compared to baseline. No changes were detected in  $\lambda_1$  ( $P = 0.027$ ),  $\lambda_2$  ( $P = 0.010$ ), or FA ( $P = 0.034$ ). Mean  $qT_2$  values ( $P = 0.003$ ) and pseudoperfusion fractions ( $P = 0.003$ ) were higher at baseline compared to follow-up.

### Local vs. Whole Muscle Values

The percentage change in MD and  $qT_2$  between the baseline and postmarathon timepoints were more pronounced locally as compared to whole muscle, with average local  $\Delta MD = 2.45\%$  (VM; range mean relative difference for segment 1–5: 1.37–3.92%) and 2.17% (BFL; range mean relative difference for segment 1–5: 0.97–3.44%) and  $\Delta qT_2 = -0.16\%$  (VM; range mean relative difference for segment 1–5: -1.02–0.83) and 1.63% (BFL; range mean relative difference for segment 1–5: -0.39 – 5.03%) vs. whole-muscle  $\Delta MD = 1.48\%$  (VM) and 1.35% (BFL) and  $\Delta qT_2 = -0.94\%$  (VM) and 0.16% (BFL). MD values were higher postmarathon compared to baseline in the VM (2/5 segments;  $P < 0.01$ ) and BFL (1/5 segments;  $P = 0.006$ ).  $qT_2$  was higher in the BFL postmarathon (1/5 segments;  $P = 0.003$ ) compared to baseline (Table 4 and Fig. 5 & 6).

## Discussion

A multiparametric quantitative MRI approach was used to assess microstructural changes in the upper leg muscles after running a marathon. Our results revealed small, but distinct, changes in quantitative MRI parameters, particularly the MRI diffusion indices, shortly after completion of the marathon in the absence of overt muscle injury. These transient changes

were accompanied by mildly elevated CK concentrations that are, among other things, indicative of exercise-induced muscle microtrauma. Changes were more pronounced in specific muscles and muscle parts, which emphasizes that microtrauma following endurance running is not homogeneously distributed across the upper legs.

RD, MD, and  $\lambda_3$  were elevated in the majority of upper legs muscles postmarathon and returned to premarathon values at follow-up, whereas  $\lambda_2$ ,  $\lambda_1$ , and FA showed a similar but less pronounced effect. These observations are in line with previous work that detected similar

transient changes in the diffusion parameters after running a marathon.<sup>5</sup> In that earlier work, however, imaging was restricted to T<sub>2</sub>-weighted MRI and DTI and did not measure plasma CK concentrations, which hampered interpretation of the observed changes in the diffusion indices. The present multiparametric approach shows that the transient changes in the diffusion indices seem intrinsic to muscle tissue microstructure and likely do not originate from contamination of the diffusion values by pseudoperfusion or edema. Moreover, no clear pattern in the pseudoperfusion and qT<sub>2</sub> values were observed, which shows that the diffusion parameters are more

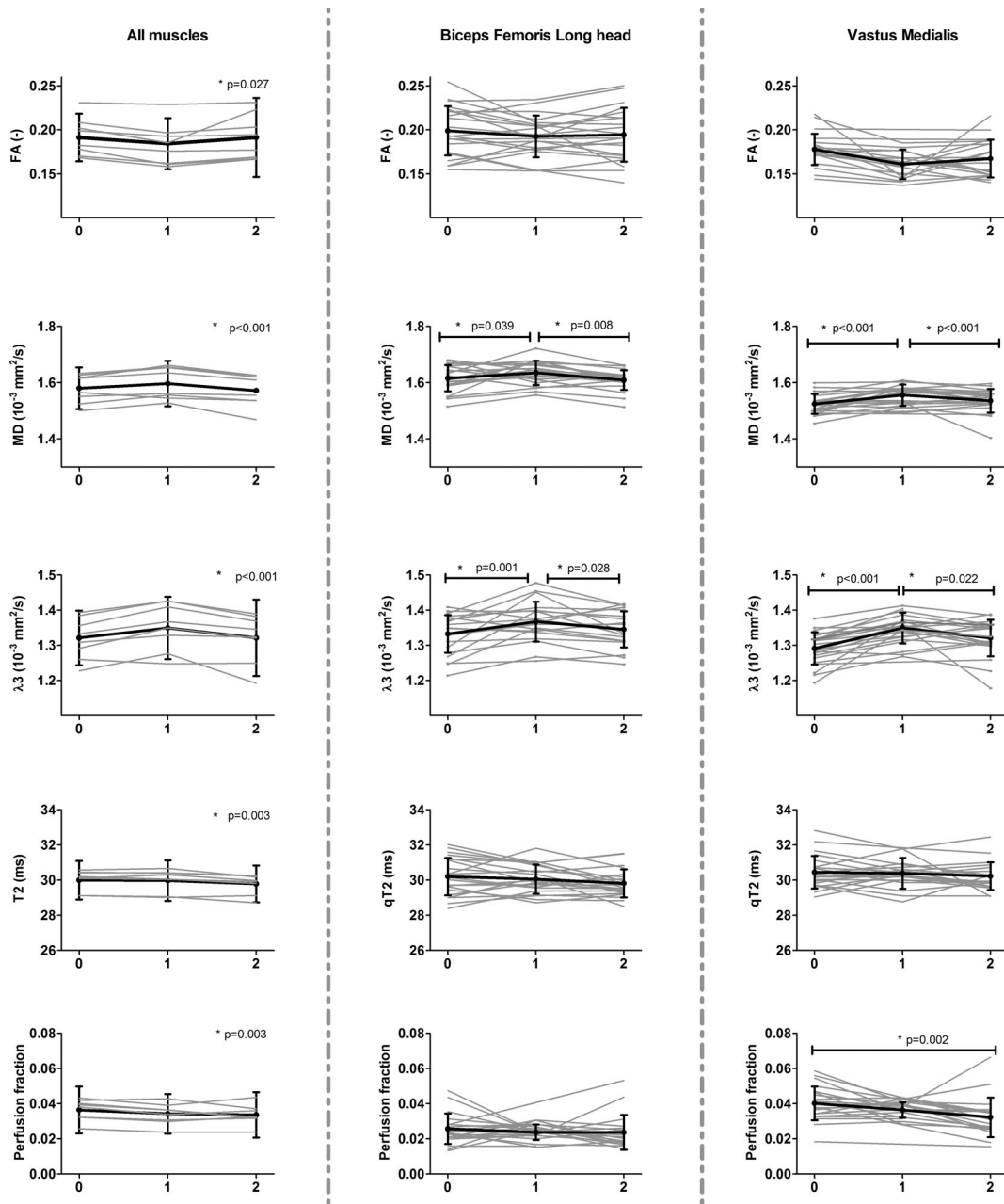


FIGURE 4: Time courses of FA, MD,  $\lambda_3$ , qT<sub>2</sub>, and perfusion fraction for all upper leg muscles separately (left and right leg taken together; left column) and for all subjects separately for the BFL and VM muscle. Each muscle (left column) or subject (middle and right column) is shown in gray, while the mean and standard deviation are shown in black. Asterisks indicate an overall time-effect in the left column and a significant change between timepoints in the middle and right column. The timepoints are defined as 0 = baseline, 1 = postmarathon, and 2 = follow-up.

**TABLE 4. Mean and Standard Deviations for the Mean Diffusivity and  $qT_2$ , for the Five Segments of BFL and VM Muscle, Per Timepoint**

Muscle	Parameter	Timepoint	Segment 1	Segment 2	Segment 3	Segment 4	Segment 5
BFL	MD	B	1.51 ± 0.09	1.57 ± 0.04	1.62 ± 0.04	1.63 ± 0.04	1.57 ± 0.06
		Post	1.55 ± 0.08	1.62 ± 0.04*	1.65 ± 0.04	1.65 ± 0.04	1.61 ± 0.04
		2-week	1.50 ± 0.09	1.55 ± 0.07	1.61 ± 0.04	1.62 ± 0.02	1.57 ± 0.04
	$qT_2$	B	30.6 ± 1.6	29.9 ± 1.25	29.7 ± 1.25	29.6 ± 1.4	29.3 ± 1.3
		Post	31.8 ± 1.6*	30.6 ± 0.9	29.9 ± 0.9	29.2 ± 1.2	29.6 ± 1.1
		2-week	31.8 ± 1.9	30.0 ± 1.2	29.5 ± 1.1	29.4 ± 0.9	29.2 ± 1
VM	MD	B	1.44 ± 0.05	1.48 ± 0.04	1.52 ± 0.05	1.59 ± 0.05	1.60 ± 0.05
		Post	1.51 ± 0.04*	1.53 ± 0.05*	1.54 ± 0.06	1.60 ± 0.04	1.60 ± 0.03
		2-week	1.50 ± 0.08	1.53 ± 0.06	1.53 ± 0.07	1.56 ± 0.05	1.58 ± 0.04
	$qT_2$	B	30.6 ± 1.55	30.5 ± 1.3	29.9 ± 1.1	29.8 ± 0.8	29.8 ± 1.0
		Post	31.1 ± 1.7	31.03 ± 1.3	30.3 ± 1.04	30.3 ± 1.11	30.1 ± 1.0
		2-week	30.9 ± 1	30.9 ± 0.8	30.2 ± 0.8	30.1 ± 0.6	30.1 ± 0.7

BFL: Biceps Femoris Long Head, VM: Vastus Medialis, MD: Mean Diffusivity,  $qT_2$ : quantitative  $T_2$  measurements, B: baseline, post: postmarathon, 2-week: follow-up. Differences between baseline and postmarathon are indicated with an asterisk (\*).

sensitive to detect the underlying muscle damage. Similarly but more pronounced DTI and  $qT_2$  changes have been reported after strenuous types of eccentric exercise, known to induce muscle strain injury.<sup>9,31–33</sup> Moreover, in these studies DTI and  $T_2$  changes showed to be maximal at 24–48 hours postexercise and recovered to baseline values within a week, while other groups evaluated the acute effects of exercise that normalized within a few hours postexercise.<sup>12,15,32,34</sup> In acute injury, it is known that changes in all the eigenvalues and FA are due to less restriction of water diffusion. Of those parameters,  $\lambda_2$  and  $\lambda_3$  are reported as the most sensitive to muscle microdamage because they symbolize the cross-fiber architecture.<sup>8,35</sup> Our results show a similar pattern for  $\lambda_3$  and a less pronounced pattern for  $\lambda_2$ , suggesting that  $\lambda_3$  is the most sensitive to muscle microdamage. Furthermore, in this work both MD and RD were increased postmarathon, largely caused by the increase in  $\lambda_3$ . However, in spite of any significant changes in the  $\lambda_1$  and  $\lambda_2$  itself, these parameters do show a similar pattern and therefore contribute to the overall diffusivity in MD and RD. Taken together, we believe that the changes in diffusion parameters postmarathon reflect subclinical damage to the myocytes. Additionally, DTI was able to detect the recovery of these transient changes in microstructure over time, which shows the prospective potential of this technique for monitoring muscle tissue repair after strain injury.

A local assessment of the muscle damage in the VM and BFL muscle revealed more pronounced effects than

whole-muscle volume averages. This heterogeneity within individual muscles needs to be considered during muscle injury evaluation. The VM diffusion indices were more homogeneously elevated along the muscle length, whereas the BFL showed a focal change in the second of five segments on the distal side of the muscle. These differences are likely related to the type of activity, as well as the specific muscle function and architecture, determining stress and strain distributions during running.<sup>21</sup> Mao et al and Kubota et al measured  $T_2$  changes after downhill running and various types of eccentric exercises in three locations along the length of the quadriceps muscles.<sup>29,33,36</sup>  $T_2$  changes were small and, in agreement with our findings, changes were heterogeneous within and between individual muscles and also varied per type of exercise.

### Limitations

Some limitations of the study should be acknowledged. First, IVIM modeling provides a good and practical way to correct the diffusion indices for perfusion contamination. However, although IVIM-derived pseudoperfusion values and perfusion fractions have been shown to correlate well with the underlying capillary perfusion, they need to be treated with some caution, since they critically depend on, among others, the type of diffusion sequence, choice of b-values, and SNR values.<sup>37</sup> Second, although the multiparametric approach used here could be performed in clinical practice, it will definitely



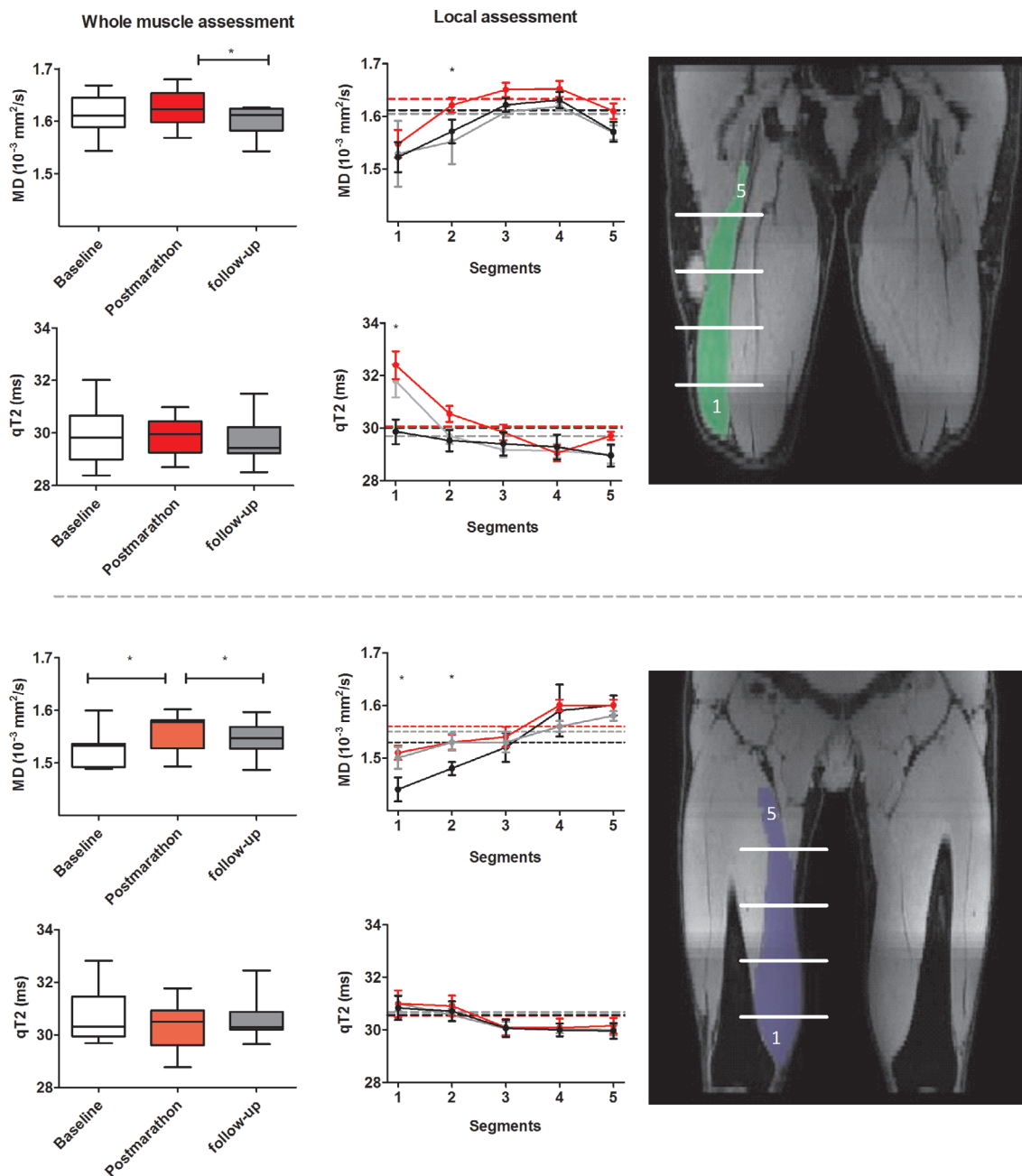


**FIGURE 5:** Comparisons between whole muscle volume and local measurements. Left: boxplots showing MD and  $qT_2$  for the BFL (top) and VM (bottom) muscle for all subjects based on a whole volume assessment. Middle: line graphs of MD and  $qT_2$  for five segments of the BFL and VM muscle averaged over all subjects at baseline (black), postmarathon (red), and follow-up (gray). Asterisks indicate significant time-effects between baseline and postmarathon. Right: showing the location of the five muscle segments for the BFL and VM muscle. Note that the difference in MD and  $qT_2$  values between timepoints is more pronounced for the localized measurements, indicating the higher sensitivity to detect changes.

benefit from a reduction in total scan duration. Both multiband imaging and different  $k$ -space under sampling techniques may be explored for acquisition acceleration.<sup>38–40</sup> Also, the manual segmentation step, which was essential for quantification of the diffusion indices and  $qT_2$  values, was time-consuming, requiring up to 8 hours for segmenting all muscles in one of the upper legs. Semiautomated and automated segmentation methods are therefore highly desired.

Additionally, blood CK concentrations are known to be affected by many factors, such as age, gender, ethnicity, and hydration status and are not necessarily specific for muscle damage.<sup>41</sup> Our statistical model accounted for any between-subject variations. However, it could be that the elevated CK concentrations detected here are related to other damage, represent general exercise effects, or a change in hydration status. Another factor that needs to be considered is the varying

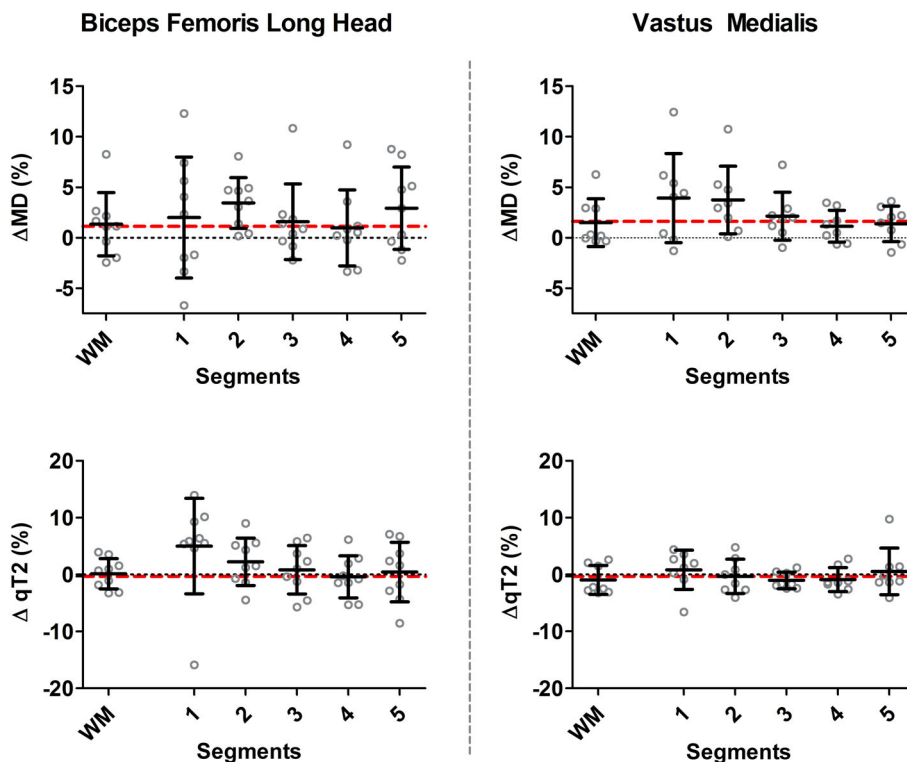


**FIGURE 6:** Comparisons between whole muscle volume and local measurements in percentage change. Scatterplots showing mean diffusivity (MD) (top) and  $qT_2$  (bottom) for the BFL (left) and VM (right) muscle for all subjects based on a whole volume assessment and the five local measurements. Relative change was determined per subject between baseline and postmarathon measurements. Each gray dot reflects the relative change between baseline and postmarathon for an individual subject, with the group mean and standard deviation shown in black. The red dotted line represents the average  $\Delta\%$  for the whole muscle volume measurements between baseline and postmarathon.

levels of experience and training regimes of the participants, which could result in different degrees of strain caused by running a marathon, introducing some heterogeneity in the data. Nonetheless, we were able to show overall diffusion changes in the majority of upper leg muscles. For practical purposes, we could only measure at two timepoints after running of the marathon, which provided only limited information on the full time course of damage and recovery. It is known that myalgia is maximal within the 24–48-hour time window following marathon running. Any microstructural changes may therefore be expected to be at maximum during our postmarathon MR examinations. Finally, the sample size of this study was small and has a relatively broad age-range. In order to avoid introducing more heterogeneity in the group due to gender and hormone cycles we focused on assessing the effect of marathon running on skeletal muscle in men. However, for future studies it would be interesting to assess if there are gender-specific effects of marathon running on skeletal muscle.

### Conclusion

This multiparametric MRI protocol, and specifically DTI, was able to detect subclinical damage (microtrauma) and

recovery after running a marathon in individual upper leg muscles and muscle locations.

### Acknowledgments

Grant Support: Dutch Technology Foundation TTW (DIMASK #15500). Sportinnovator grant of The Netherlands Organization for Health Research and Development, ZonMw (#50-53800-98-PR020).

### References

- Ekstrand J, Hägglund M, Waldén M. Epidemiology of muscle injuries in professional football (soccer). *Am J Sports Med* 2011;39(6):1226-1232. <https://doi.org/10.1177/0363546510395879>.
- Faulkner JA, Brooks SV, Opitck JA. Injury to skeletal muscle fibers during contractions: Conditions of occurrence and prevention. *Phys Ther* 1993;73(12):911-921.
- Armstrong RB. Mechanisms of exercise-induced delayed onset muscular soreness: A brief review. *Med Sci Sports Exerc* 1984;16(6):529-538.
- Wan B, Shan G. Biomechanical modeling as a practical tool for predicting injury risk related to repetitive muscle lengthening during learning and training of human complex motor skills. *Springerplus* 2016;5:441.
- Froeling M, Oudeman J, Strijkers GJ, et al. Muscle changes detected with diffusion-tensor imaging after long-distance running. *Radiology* 2014;274(2):548-562.

6. Reurink G, Brilman EG, de Vos RJ, et al. Magnetic resonance imaging in acute hamstring injury: Can we provide a return to play prognosis? *Sports Med* 2014;45(1):133-146.
7. Heiderscheidt BC, Sherry MA, Silder A, Chumanov ES, Thelen DG. Hamstring strain injuries: Recommendations for diagnosis, rehabilitation, and injury prevention. *J Orthop Sports Phys Ther* 2010;40(2):67-81.
8. Zaraiskaya T, Kumbhare D, Noseworthy MD. Diffusion tensor imaging in evaluation of human skeletal muscle injury. *J Magn Reson Imaging* 2006;24(2):402-408.
9. Yanagisawa O, Kurihara T, Kobayashi N, Fukubayashi T. Strenuous resistance exercise effects on magnetic resonance diffusion parameters and muscle-tendon function in human skeletal muscle. *J Magn Reson Imaging* 2011;34(4):887-894.
10. Nakai R, Azuma T, Sudo M, Urayama S, Takizawa O, Tsutsumi S. MRI analysis of structural changes in skeletal muscles and surrounding tissues following long-term walking exercise with training equipment. *J Appl Physiol* 2008;105(3):958-963.
11. Fulford J, Eston RG, Rowlands AV, Davies RC. Assessment of magnetic resonance techniques to measure muscle damage 24 h after eccentric exercise. *Scand J Med Sci Sport* 2015;25(1):e28-e39.
12. Morvan D, Leroy-Willig A. Simultaneous measurements of diffusion and transverse relaxation in exercising skeletal muscle. *Magn Reson Imaging* 1995;13(7):943-948.
13. Takahashi H, Kuno SYA, Miyamoto T, et al. Changes in magnetic resonance images in human skeletal muscle after eccentric exercise. *Eur J Appl Physiol Occup Physiol* 1994;69(5):408-413.
14. Shellock FG, Fukunaga T, Mink JH, Edgerton VR. Exertional muscle injury: Evaluation of concentric versus eccentric actions with serial MR imaging. *Radiology* 1991;179(3):659-664.
15. Ababneh ZQ, Ababneh R, Maier SE, et al. On the correlation between T2 and tissue diffusion coefficients in exercised muscle: Quantitative measurements at 3T within the tibialis anterior. *Magn Reson Mater Phys, Biol Med* 2008;21(4):273-278.
16. Damon BM. Effects of image noise in muscle diffusion tensor (DT)-MRI assessed using numerical simulations. *Magn Reson Med* 2008;60(4):934-944.
17. Le Bihan D, Breton E, Lallemand D, Grenier P, Cabanis E, Laval-Jeantet M. MR imaging of intravoxel incoherent motions: Application to diffusion and perfusion in neurologic disorders. *Radiology* 2014;161(2):401-407.
18. Hazlewood CF, Chang DC, Nichols BL, Woessner DE. Nuclear magnetic resonance transverse relaxation times of water protons in skeletal muscle. *Biophys J* 1974;14(8):583-606.
19. Hooijmans MT, Niks EH, Burakiewicz J, et al. Non-uniform muscle fat replacement along the proximodistal axis in Duchenne muscular dystrophy. *Neuromuscul Disord* 2017;27(5):458-464.
20. Schlaffke L, Rehmann R, Froeling M, et al. Diffusion tensor imaging of the human calf: Variation of inter- and intramuscle-specific diffusion parameters. *J Magn Reson Imaging* 2017;46(4):1137-1148.
21. Shin DD, Hodgson JA, Edgerton VR, Sinha S. In vivo intramuscular fascicle-aponeuroses dynamics of the human medial gastrocnemius during plantarflexion and dorsiflexion of the foot. *J Appl Physiol* 2009;107(4):1276-1284.
22. Boss A, Heskamp L, Breukels V, Bains LJ, van Uden MJ, Heerschap A. Oxidative capacity varies along the length of healthy human tibialis anterior. *Physiology* 2018;596(8):1467-1483.
23. Friedenreich CM, Courneya KS, Bryant HE. The lifetime total physical activity questionnaire: Development and reliability. *Med Sci Sports Exerc* 1998;30(2):266-274.
24. Schlaffke L, Rehmann R, Rohm M, et al. Multi-center evaluation of stability and reproducibility of quantitative MRI measures in healthy calf muscles. *NMR Biomed* 2019;32(9):e4119.
25. De Luca A, Bertoldo A, Froeling M. Effects of perfusion on DTI and DKI estimates in the skeletal muscle. *Magn Reson Med* 2017;78(1):233-246.
26. Marty B, Baudin P-Y, Reyngoudt H, et al. Simultaneous muscle water T2 and fat fraction mapping using transverse relaxometry with stimulated echo compensation. *NMR Biomed* 2016;29(4):431-443.
27. Mueller-Wohlfahrt HW, Haensel L, Mithoefer K, et al. Terminology and classification of muscle injuries in sport: The Munich consensus statement. *Br J Sports Med* 2013;47(6):342-350.
28. Froeling M, Nederveen AJ, Nicolay K, Strijkers GJ. DTI of human skeletal muscle: The effects of diffusion encoding parameters, signal-to-noise ratio and T2 on tensor indices and fiber tracts. *NMR Biomed* 2013;26(11):1339-1352.
29. Maeo S, Ando Y, Kanehisa H, Kawakami Y. Localization of damage in the human leg muscles induced by downhill running. *Sci Rep* 2017;7(1):5769.
30. Brukner P, Connell D. "Serious thigh muscle strains": Beware the intramuscular tendon which plays an important role in difficult hamstring and quadriceps muscle strains. *Br J Sports Med*. 2016;50(4):205-208.
31. Sigmund EE, Baete SH, Patel K, et al. Spatially resolved kinetics of skeletal muscle exercise response and recovery with multiple echo diffusion tensor imaging (MEDITI): A feasibility study. *Magn Reson Mater Phys, Biol Med* 2018;31(5):599-608.
32. Nygren AT, Kaijser L. Water exchange induced by unilateral exercise in active and inactive skeletal muscles. *J Appl Physiol* 2002;93(5):1716-1722.
33. Maeo S, Saito A, Otsuka S, Shan X, Kanehisa H, Kawakami Y. Localization of muscle damage within the quadriceps femoris induced by different types of eccentric exercises. *Scand J Med Sci Sport* 2018;28(1):95-106.
34. Keller S, Yamamura J, Sedlacik J, et al. Diffusion tensor imaging combined with T2 mapping to quantify changes in the skeletal muscle associated with training and endurance exercise in competitive triathletes. *Eur Radiol* 2020 [epub ahead of print]. <https://doi.org/10.1007/s00330-019-06576-z>.
35. Giraudo C, Motyka S, Weber M, Feiweier T, Trattng S, Bogner W. Diffusion tensor imaging of healthy skeletal muscles: A comparison between 7T and 3T. *Invest Radiol* 2019;54(1):48-54.
36. Kubota J, Ono T, Araki M, Torii S, Okuwaki T, Fukubayashi T. Non-uniform changes in magnetic resonance measurements of the semitendinosus muscle following intensive eccentric exercise. *Eur J Appl Physiol* 2007;101(6):713-720.
37. Adelnia F, Shardell M, Bergeron CM, et al. Diffusion-weighted MRI with intravoxel incoherent motion modeling for assessment of muscle perfusion in the thigh during post-exercise hyperemia in younger and older adults. *NMR Biomed* 2019;32(5):e4072.
38. Loughran T, Higgins DM, McCallum M, Coombs A, Straub V, Hollingsworth KG. Improving highly accelerated fat fraction measurements for clinical trials in muscular dystrophy: Origin and quantitative effect of R2\* changes. *Radiology* 2015;275(2):570-578.
39. Hollingsworth KG. Reducing acquisition time in clinical MRI by data undersampling and compressed sensing reconstruction. *Phys Med Biol* 2015;60(21):R297-R322.
40. Filli L, Piccirelli M, Kenkel D, et al. Simultaneous multislice echo planar imaging with blipped controlled aliasing in parallel imaging results in higher acceleration: A promising technique for accelerated diffusion tensor imaging of skeletal muscle. *Invest Radiol* 2015;50(7):456-463.
41. Baird MF, Graham SM, Baker JS, Bickerstaff GF. Creatine-kinase- and exercise-related muscle damage implications for muscle performance and recovery. *J Nutr Metab* 2012;2012:960363.